

Non-linear MHD Simulations of Pellet Triggered ELMs

S. Futatani^{1,2}, G.T.A. Huijsmans³, A. Loarte⁴, S. Pamela⁵, M. Hoelzl⁶, P.T. Lang⁶, L. Garzotti⁵, G. Kocsis⁷, F. Orain⁶, D. Frigione⁸, M. Dunne⁶, A. Lessig⁶, M. Mantsinen^{1,9}, EUROfusion MST1 Team, ASDEX Upgrade Team, JET Contributors¹⁰

¹Barcelona Supercomputing Center (BSC-CNS), c/ Jordi Girona 29, 08034 Barcelona, Spain

²EUROfusion Consortium, JET, Culham Science Centre, Abingdon, OX14 3DB, UK

³CEA, IRFM, F-13108, St-Paul-Lez-Durance, France

⁴ITER Organization, Route de Vinon-sur-Verdon, CS 90 046, 13067 St. Paul Lez Durance Cedex, France

⁵EURATOM/CCFE, Fusion Association, Culham Science Centre, Abingdon, Oxon OX14 3DB, UK

⁶Max Planck Institute for Plasma Physics, Boltzmannstr. 2, 85748 Garching, Germany

⁷Wigner RCP RMI, Budapest, Hungary

⁸Unità Tecnica Fusione, ENEA C.R. Frascati, via E. Fermi 45, 00044 Frascati (Roma), Italy

⁹ICREA, Barcelona, Spain

¹⁰See the author list of "Overview of the JET results in support to ITER" by X. Litaudon et al. to be published in Nuclear Fusion Special issue: Overview and summary reports from the 26th Fusion Energy Conference (Kyoto, Japan, 17-22 October 2016)

Abstract

Edge localized mode (ELM) triggered by pellet injection in the ASDEX Upgrade and JET tokamaks has been simulated with the non-linear MHD code JOEK with a view to validating its physics models for implication for ITER 15MA Q=10 operation scenarios. The computational domain covers the X-point geometry, open field lines and divertor. Regarding the JET discharge simulation, the pellet is injected after the spontaneous ELM simulation which allows to compare the power deposition profiles of spontaneous and pellet triggered ELM. The dependence of the pellet injection geometry has been studied and it is found that pellet injection from High Field Side (HFS) eases the pellet ELM triggering. The dependence of the power deposition asymmetry on the injection geometry and the consequences for ITER with the JOEK simulation of JET (#84690) which confirms the result will be presented. The particle and the energy loss during the full ELM cycle of pellet triggered ELM is also presented.

Introduction

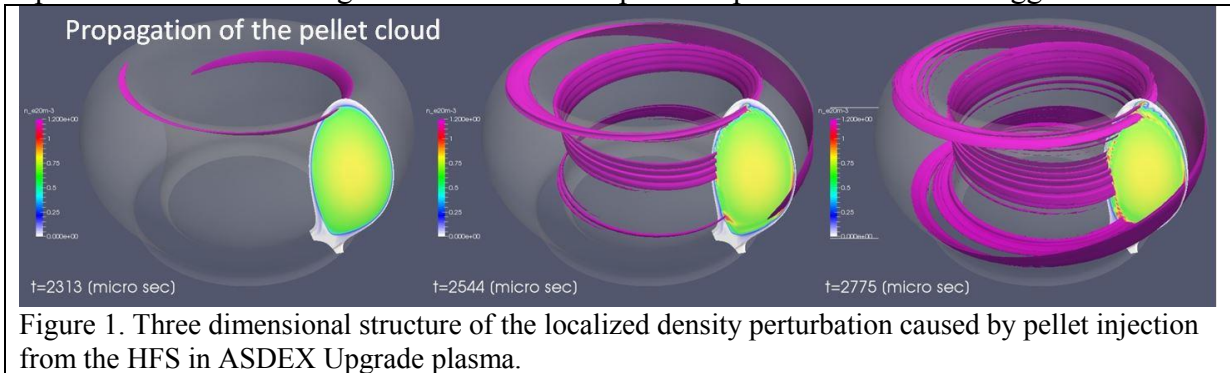
ITER operation in its high fusion performance DT scenarios relies on the achievement of the H-mode confinement regime, which is expected to lead to the quasi-periodic triggering of ELMs (Edge Localized Modes). The energy fluxes associated with spontaneous ELMs are expected to produce excessive erosion and/or superficial surface damage on the plasma facing components. Controlled triggering of ELMs by the injection of small pellets (small deuterium ice bodies) at frequencies significantly exceeding those of uncontrolled ELMs is one of the foreseen schemes to control ELM energy losses and divertor power fluxes in ITER. Although the technique has been demonstrated to decrease ELM size successfully in ASDEX Upgrade [1], JET [2], and DIII-D [3], uncertainties still remain regarding the physics understanding as well as of the consequence of its application, such as localised power loads associated with this technique [4]. Moreover, pellets may fail to trigger ELM for plasma scenarios in all metal wall ASDEX Upgrade which also requires better understanding of the underlying physical processes of the ELM triggering [8]

Modelling of ELM triggering by pellet injection for JET (#84690), ASDEX Upgrade (#29178) discharges, and ITER 15MA Q=10 scenario has been carried out with the non-linear MHD code JOEK [5, 6]. JOEK allows to determine the energy and particle

losses by the pellet triggered ELM. Regarding the JET discharge simulation, the pellet is injected after the spontaneous ELM simulation which allows to compare the power deposition profiles of spontaneous and pellet triggered ELM.

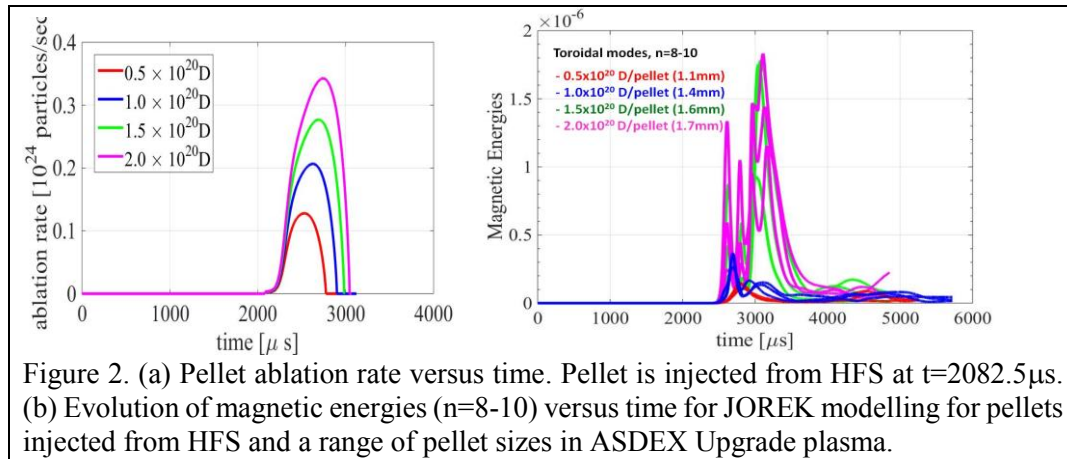
The implementation of the pellet modelling in JOREK

The non-linear MHD code JOREK includes a model for the density source coming from the ablation of an injected deuterium pellet [5, 6]. The pellet is assumed to travel along a straight line with a given fixed velocity. The amplitude of the space and time varying density source is such that the integrated source rate is consistent with the NGS (Neutral Gas Shielding) pellet ablation model [7]. With non-linear MHD equations, the pellet ablation process is calculated self-consistently. The ablation of the pellet as it travels into the plasma causes a large local, moving density source. The density source creates a density perturbation which propagates along the magnetic field line with the sound speed as shown in Fig.1. Since the deuterium pellet injection is mostly adiabatic, the temperature at the location of the density source will drop such that the local pressure stays constant initially. Due to the large heat conductivity, the region over which the density perturbation extends will be quickly heated up. This results in a strong local increase of the pressure perturbation which triggers an ELM.

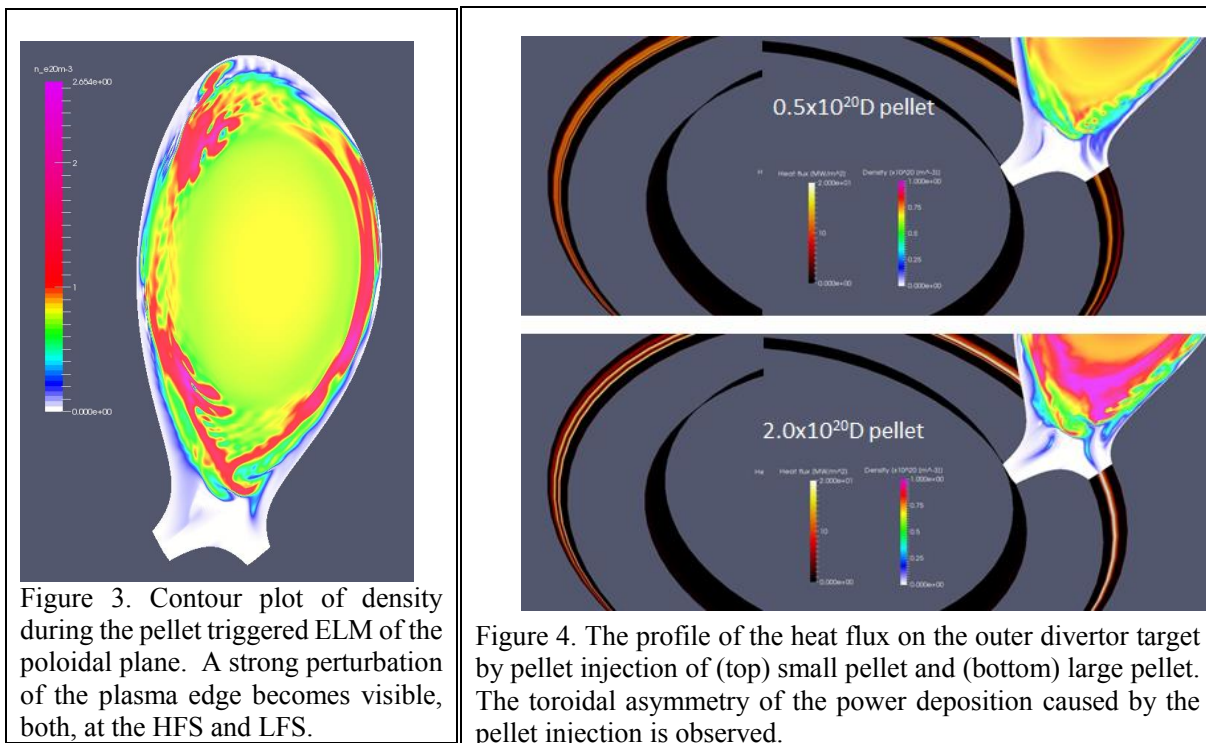


Modelling of pellet ELM triggering of ASDEX Upgrade plasma

The initial profiles for the modelling are extracted from the shot #29178 of the ASDEX Upgrade experiment. Plasma operation parameters are the plasma current of $I_p = 1.0$ MA, the toroidal magnetic field $B_T = 2.5$ T, NBI heating power $P_{NBI} = 5.2$ MW. Simulations have been carried out for pellet injection from the High Field Side (HFS) of the device [8]. The pellet size (initial pellet particle content) is varied in four steps such as 0.5×10^{20} D, 1.0×10^{20} D, 1.5×10^{20} D and 2.0×10^{20} D. The pellet ELM triggering dependence on the pellet size has been investigated keeping the injection velocity constant 240 m/s. JOREK simulations show that the pellet ablation leads to a growth of the MHD activity as reflected by the growth of kinetic and magnetic energy of the toroidal modes of $n=1-10$ as shown in Fig.2. For a small pellet size, smaller than 1.0×10^{20} D, the MHD activity decreases after the pellet is fully ablated and the pressure perturbation decreases as a consequence of the particle and energy transport processes. For large pellets, larger than 1.5×10^{20} D, a strong increase of the energy of the high toroidal modes, $n > 8$ harmonics is observed in the simulations. The strong growth of the magnetic energy above a critical pellet size, corresponding to the growth of $n=8-10$ modes is interpreted as the ELM triggering by the pellet. Figure 3 shows the density contour of the poloidal plane during an ELM triggered by a large pellet (2.0×10^{20} D). A strong perturbation of the plasma edge becomes visible, both, at the HFS and LFS.



A toroidal asymmetry of the power deposition caused by the pellet injection is observed as shown in Fig. 4. This is consistent with the findings of DIII-D [6], and also with the modelling of JET plasma as shown in the next paragraph. The JOREK modelling shows



the time delay between the pellet arrival into the confined plasma and the ELM triggering is about $170 \mu\text{s}$. Figure 5 (a) shows the time evolution of the energy content in the plasma versus time. Regarding the ELM size, the small pellet ($0.5 \times 10^{20}\text{D}$) causes losses of 0.38% of the total energy in $690 \mu\text{s}$, and the large pellet ($2.0 \times 10^{20}\text{D}$) causes losses 2.4% of the total energy in $1240 \mu\text{s}$. Pellet triggered ELM in the modelling is shorter and smaller than in experiment, where 10% of the plasma energy is lost in 3 ms with the injection of $1.5 \times 10^{20}\text{D}$ pellet with 259 m/s [8]. This could result from an underestimation of pedestal profiles in the equilibrium reconstruction or the lacking diamagnetic flows in simulations. Figure 5 (b) shows the energy loss of the plasma versus pellet size. The energy loss does not have a linear scaling according to the injected pellet size. The scaling of the energy loss versus pellet size

changes between the pellet size of $1.0 \times 10^{20} \text{D}$ and $1.5 \times 10^{20} \text{D}$. The threshold of the pellet size could be an identification of the minimum pellet size to trigger an ELM. The small pellets ($< 1.0 \times 10^{20} \text{D}$) do not trigger an ELM, therefore the energy loss due to the pellet triggered ELM is small. The large pellets ($> 1.5 \times 10^{20} \text{D}$) trigger an ELM, therefore the energy loss is larger than the small pellet injection.

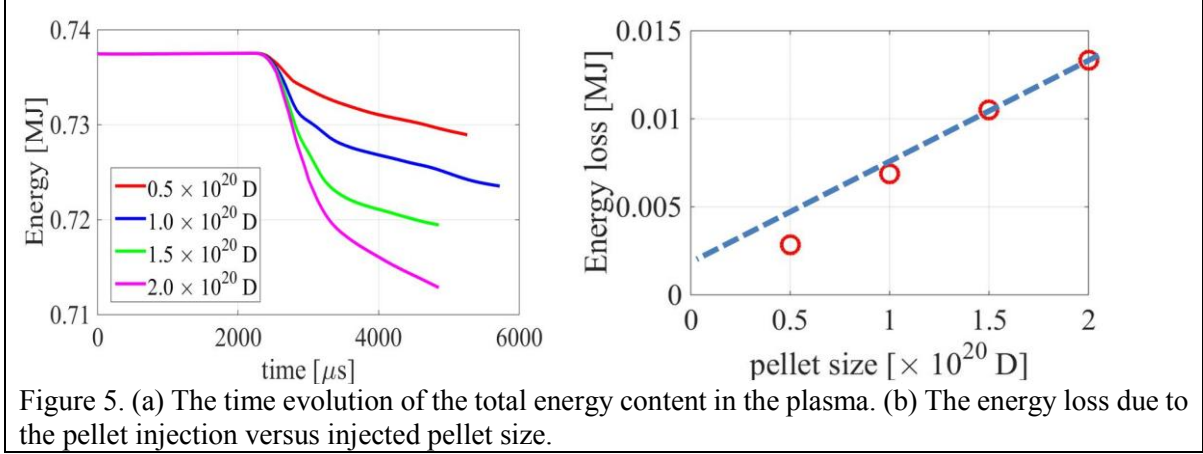


Figure 5. (a) The time evolution of the total energy content in the plasma. (b) The energy loss due to the pellet injection versus injected pellet size.

Modelling of pellet ELM triggering of JET plasma

The initial profiles for the modelling are extracted from the shot of #84690 of the JET experiment. The plasma was a baseline H-mode scenario with toroidal magnetic field $B_T = 2.1 \text{ T}$, plasma current $I_p = 2.4 \text{ MA}$, and NBI heating power $P_{\text{NBI}} = 10.5 \text{ MW}$. Simulations have been carried out for pellet injection from the outer midplane of the device which corresponds to the work of Ref [9]. Four pellet sizes have been studied; $0.25 \times 10^{20} \text{D}$, $0.5 \times 10^{20} \text{D}$, $2.0 \times 10^{20} \text{D}$ and $3.5 \times 10^{20} \text{D}$. The pellet injection velocity is fixed to 78 m/s. Regarding the JET discharge simulation, the pellet is injected after the spontaneous ELM simulation which

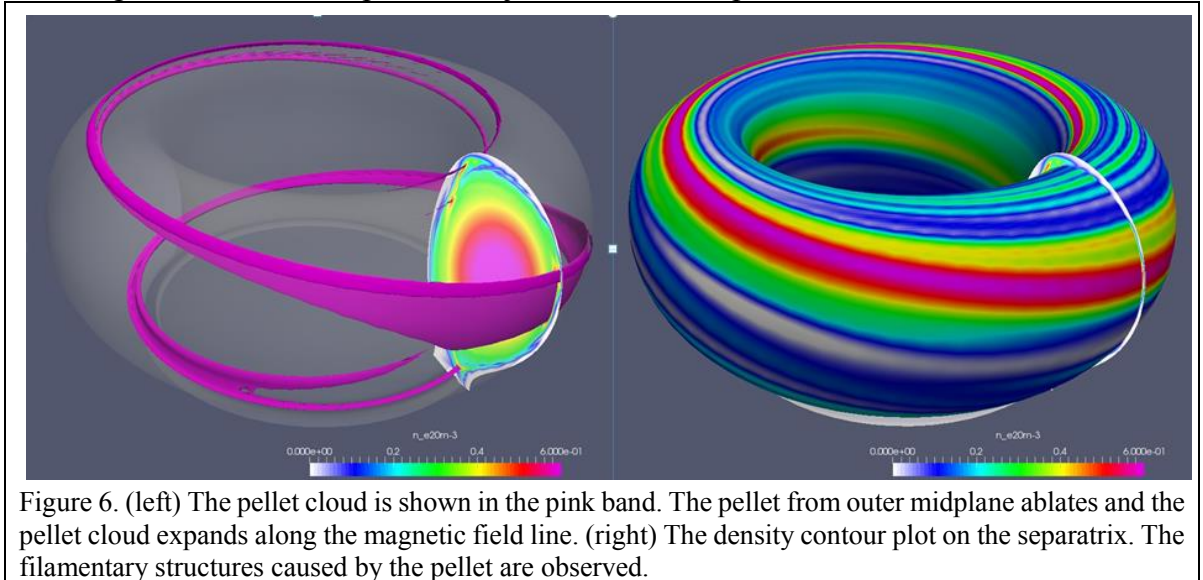
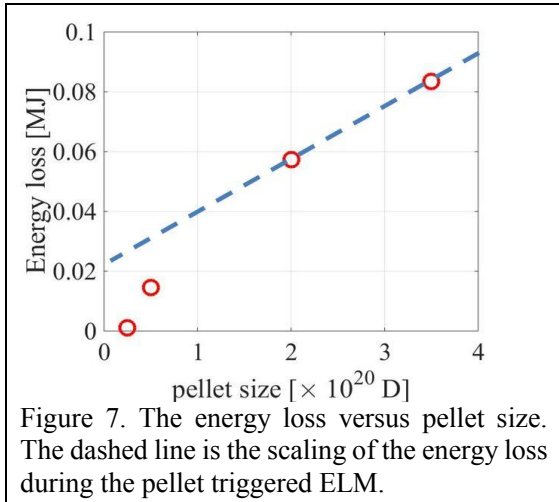


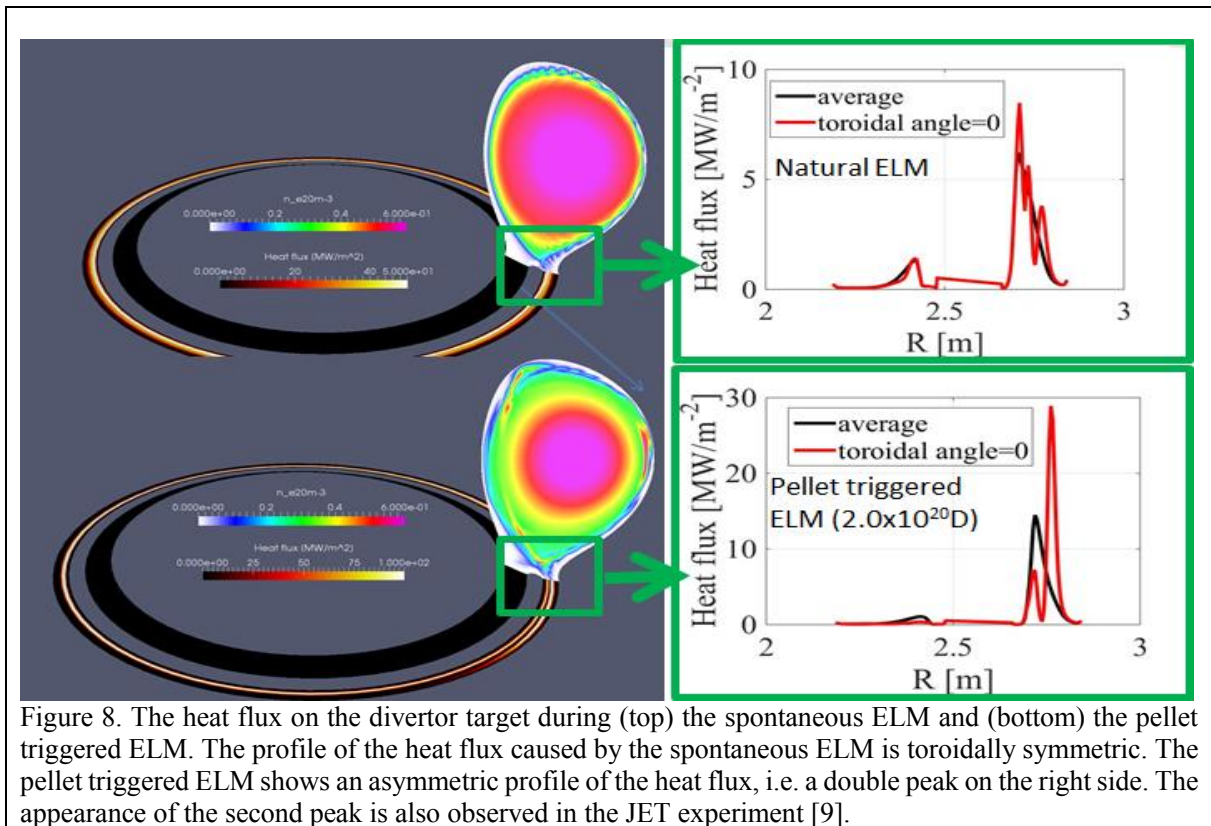
Figure 6. (left) The pellet cloud is shown in the pink band. The pellet from outer midplane ablates and the pellet cloud expands along the magnetic field line. (right) The density contour plot on the separatrix. The filamentary structures caused by the pellet are observed.

allows to compare the power deposition profiles of spontaneous and pellet triggered ELM. The JOREK simulation has been launched without pellet injection, i.e. simulation of the spontaneous ELM. When the spontaneous ELM crash occurs, the profiles of the density and the pressure are relaxed because of the particle release. The simulation of spontaneous ELM has been continued for a full ELM cycle, i.e. until the particle and energy loss stop, up to $t=15415 \mu\text{s}$. Thereafter, the pellet is injected. This approach corresponds to the pellet

injection in the early phase of the ELM cycle, i.e. just after the previous ELM crash, therefore the plasma is far from the stability limit. The JOREK simulations show that the small pellet (0.5×10^{20} D) does not trigger an ELM but the large pellet (2.0×10^{20} D) triggers an ELM. The filamentary structures caused by the large pellet (2.0×10^{20} D) injection are observed as shown in Fig.6. The width of the filamentary structures is not homogeneous as the pellet injection breaks the toroidal symmetry of the plasma. This is one of the characteristics of the pellet triggered ELM.



Regarding the ELM size of the spontaneous ELM in the JOREK modelling, the plasma loses 12% of the total energy in 9 ms. The time delay between the pellet ablation onset and the ELM triggering is about 390 μ s. Figure 7 shows the energy loss versus pellet size. The energy loss does not have a linear dependence on the pellet size which is the similar observation from ASDEX Upgrade study. The small pellet (0.5×10^{20} D) does not trigger an ELM, therefore, the energy loss is small. The large pellets ($> 2.0 \times 10^{20}$ D) trigger an ELM which leads large energy loss.



The difference comparison of the heat flux on the divertor tiles in the case of spontaneous and pellet triggered ELM have been investigated. Figure 8 shows the heat flux on the divertor target during (top) the spontaneous ELM and (bottom) the pellet triggered ELM. The comparison between spontaneous and pellet triggered ELM on the profiles of the heat flux looks that the pellet triggered ELM causes a peak about three times larger than the spontaneous ELM, although the ELM is induced far from the stability limit of the pedestal. In the modelling, the pellet triggered ELM leads to smaller energy losses than the spontaneous ELM, but also on a much shorter time scale. These observations not fully in line with experimental observations are currently under investigation. The profile of the heat flux caused by the spontaneous ELM is toroidally symmetric. On the other hand, the pellet triggered ELM shows an asymmetric profile of the heat flux, i.e. a double peak on the toroidal side of the pellet injection. The second peak grows during the pellet triggered ELM. After the termination of the pellet ablation, the ELM behaviour relaxes and the second peak of the heat flux shrinks back. The appearance of the second peak is also observed in the JET experiment [4, 9]. The secondary peak of the heat flux is due to the density perturbation at the X-point region as shown in Fig. 9. The density perturbation due to the pellet ablation creates a secondary connection of the particle/heat flux on the divertor target.

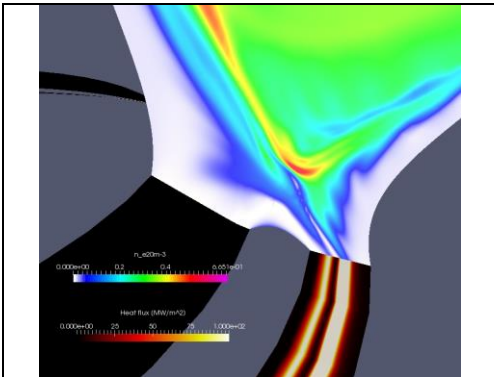


Figure 9. The density contour and the heat flux on the divertor target. The density perturbation due to the pellet ablation creates a secondary connection of the particle/heat flux on the divertor target.

Modelling of pellet ELM triggering of ITER 15MA Q=10 plasma operation scenario

JOREK simulations of pellet triggering of ELMs has been carried out for typical conditions of a 15MA Q=10 plasma as modelled with CORSICA [10]. CORSICA is a package which combines a 2D free boundary equilibrium package with various transport and source models. The pellet requirements for ELM triggering in ITER in the foreseen injection geometry (Xpoint injection, see Fig. 9), corresponding to the design specification of the ITER system [11] have been studied. Three cases of the pedestal top have been studied, 150kPa, 112.5kPa

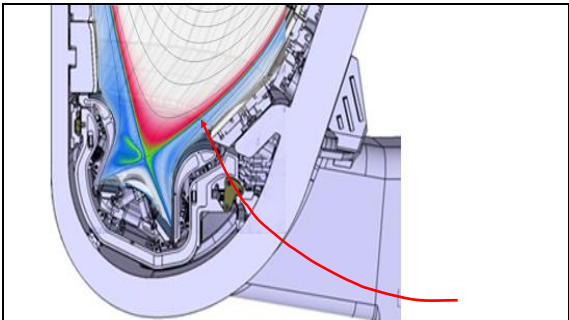


Figure 9. Pellet injection geometry foreseen in ITER for ELM pellet pacing

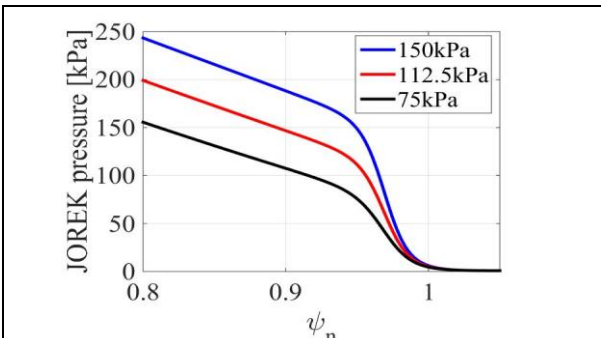


Figure 10. Pressure profiles of the plasma equilibrium for three cases of pedestal top, 150kPa, 112.5kPa and 75kPa.

and 75kPa. The case of 150kPa is unstable

which leads large spontaneous ELM while the 75kPa case is very stable. 112kPa case is the marginal between the stable and unstable condition.

JOREK pellet modelling has been performed with the most stable plasma, the case of 75kPa of the pedestal top. Three pellet sizes/particle contents (1.0×10^{21} , 2.0×10^{21} and 4.0×10^{21} particles per pellet corresponding to cylindrical pellet sizes of 2.3mm, 3.0mm and 4.7mm respectively) have been studied with the injection velocity of 300m/s. The largest pellet, 4.7mm pellet triggers an ELM and clear ballooning mode structures are observed as shown in Figure 11. The dependence of the power deposition asymmetry caused by pellet injection is also observed as shown in Fig. 12. This is consistent with the findings of DIII-D [6], ASDEX Upgrade and JET of this work.

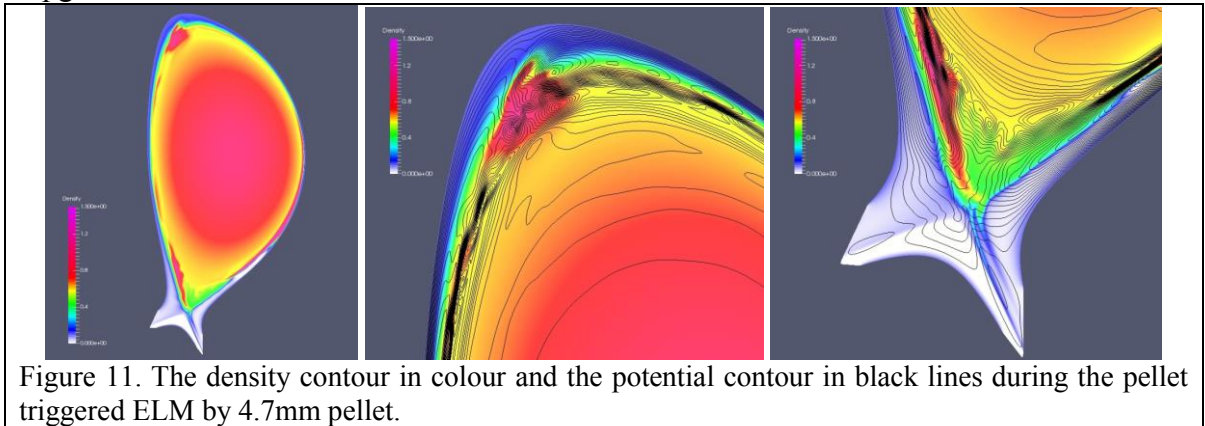


Figure 11. The density contour in colour and the potential contour in black lines during the pellet triggered ELM by 4.7mm pellet.

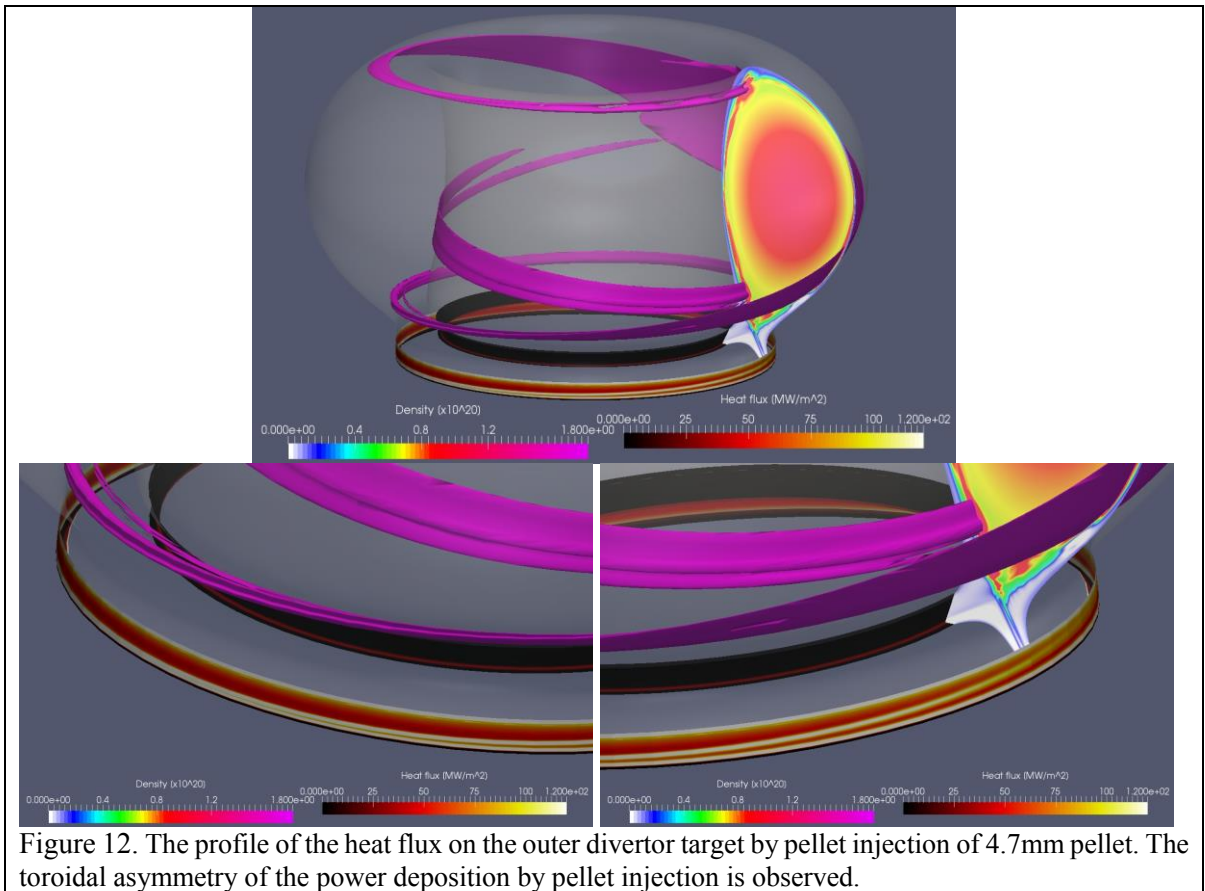


Figure 12. The profile of the heat flux on the outer divertor target by pellet injection of 4.7mm pellet. The toroidal asymmetry of the power deposition by pellet injection is observed.

Keeping the same pellet size, 2.0×10^{21} D/pellet (3.0mm cylindrical pellet) has been injected in the plasma of 75kPa pedestal top and 112.5kPa pedestal top in order to estimate the distance of the plasma stability limit. Figure 13 shows the energy content in the plasma versus time of the plasma of 75kPa and 112.5kPa. The 3.0mm pellet injection in 75kPa plasma also leads the energy loss in the 75kPa pedestal top plasma. It leads 0.15% of the total energy loss in 0.1ms. The 3.0mm pellet injected in 112.5kPa plasma leads larger energy loss, 0.2% of the total energy in 0.1ms, which is factor 2 larger than the case of 75kPa.

Conclusion

The non-linear MHD simulations of pellet ELM triggering have been performed with JOREK code. The pellet size which is sufficient to trigger an ELM is estimated by the numerical modelling for ASDEX Upgrade and JET plasma. The demonstration of the pellet ELM triggering in ITER 15MA $Q=10$ scenario plasma has been carried out. The power deposition asymmetry due to the pellet ELM triggering has been studied. The braking of the toroidal symmetry in the heat flux profile is observed, similar to the DIII-D study [6]. The JOREK modelling shows some qualitative agreement with the experiment but needs to be extended for future work by including diamagnetic, neoclassical, and toroidal flows in the simulations to allow for a more quantitative comparison. For ASDEX Upgrade, comparisons of spontaneous [12] and pellet-triggered ELMs are planned for the near future.

Acknowledgements

This work has been carried out within the framework of the EUROfusion Consortium and has received funding from the Euratom research and training programme 2014-2018 under grant agreement No 633053. The part of the work was carried out using the HELIOS supercomputer system at Computational Situational Centre of International Fusion Energy Research Centre (IFERC-CSC), Aomori, Japan, under the Broader Approach collaboration between Euratom and Japan, implemented by Fusion for Energy and JAEA. We acknowledge PRACE for awarding us access to resource Mare Nostrum based in Spain at Barcelona. The author thankfully acknowledges the computer resources, technical expertise and assistance provided by the Red Española de Supercomputación. The views and opinions expressed herein do not necessarily reflect either those of the European Commission or those of the ITER Organization.

References

[1] P. Lang et al., Nucl. Fusion **44** 665 (2004). [2] P. Lang et al., Nucl. Fusion **53** (2013) 073010. [3] L. Baylor et al., Phys. Rev. Lett. **110** (2013) 245001. [4] R. Wenninger et al., Plasma Phys. Control. Fusion **53** (2011) 105002. [5] G.T.A. Huysmans and O. Czarny, Nucl. Fusion **47**, 659 (2007). [6] S. Futatani et al., Nucl. Fusion **54**, 073008 (2014). [7] K. Gal et al., Nucl. Fusion **48**, 085005 (2008). [8] P. Lang et al., Nucl. Fusion **54**, 083009 (2014). [9] D. Frigione et al., J. Nucl. Materials **463**, 714 (2015). [10] T. Casper et al., Nucl. Fusion **54**, 013005 (2014). [11] Maruyama S. et al., 2012 24th Fusion Energy Conf. (San Diego, CA, 2012) paper ITR/P5-24 and www-naweb.iaea.org/napc/physics/FEC/FEC2012/index.htm [12] I. Krebs et al., Phys. Plasmas, **20**, 082506 (2013).

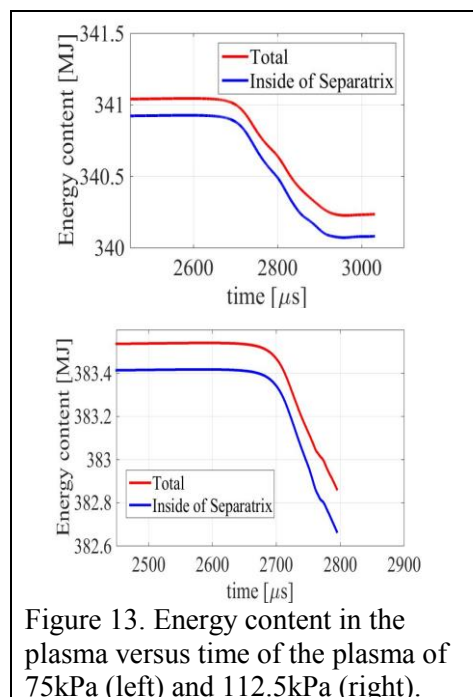


Figure 13. Energy content in the plasma versus time of the plasma of 75kPa (left) and 112.5kPa (right).